

Tunable Chiral Bound States in a Dimer Chain of Coupled Resonators

Jing Li,¹ Jing Lu,¹ Z. R. Gong,^{2,*} and Lan Zhou^{1,†}

¹*Synergetic Innovation Center for Quantum Effects and Applications,
Key Laboratory for Matter Microstructure and Function of Hunan Province,
Key Laboratory of Low-Dimensional Quantum Structures and Quantum Control of Ministry of Education,
School of Physics and Electronics, Hunan Normal University, Changsha 410081, China*

²*College of Physics and Optoelectronic Engineering, Shenzhen University, Shenzhen 518060, P. R. China*

(Dated: September 1, 2023)

We study an excitation hopping on a one-dimensional (1D) dimer chain of coupled resonators with the alternate on-site photon energies, which interacts with a two-level emitter (TLE) by a coupling point or two adjacent coupling points. In the single-excitation subspace, this system not only possesses two energy bands with propagating states, but also possesses photonic bound states. The number of bound states depends on the coupling forms between the TLE and the dimer chain. It is found that when the TLE is locally coupled to one resonator of the dimer chain, the bound-state has mirror reflection symmetry. When the TLE is nonlocally coupled to two adjacent resonators, three bound states with preferred direction arise due to the mirror symmetry breaking. By using chirality to measure the asymmetry, it is found that the chirality of these bound states can be tuned by changing the energy differences of single photon in the adjacent resonators, the coupling strengths and the transition energy of the TLE.

I. INTRODUCTION

The quantum electrodynamics of light-matter interactions in waveguide systems [1–3] has attracted considerable interest. In a waveguide, the electromagnetic field is confined spatially in two dimensions and propagates along the remaining one, which is called guided modes. The interference of spontaneously emitted waves from a quantum emitter (QE) and the incident wave leads to total reflection of single photons in the one-dimensional (1D) waveguide with linear [4] or nonlinear [5] dispersion relation. One of the most intriguing is the existence of bound states for photons: the single-photon bound states in continuum [6–9], where the photon is trapped between the QEs or the mirror and a QE; the single-photon bound states with energies slightly outside the continuum [10–16], where a photon is localized and symmetrical around the resonator coupling to the quantum emitter; multiple-photon bound states [17–21], which give rise to strong correlations between photons.

Nowadays, widespread attention has been paid on giant atoms. Different from a local interaction between QEs and light field [22–29], giant atoms nonlocally couples to light field [30–37] at multiple points. Such unconventional light-matter interaction occurs when the atomic size is comparable or even larger than the wavelength of the light. The interference effects between these multiple coupling points leads to unconventional phenomenon such as frequency dependent relaxation and Lamb shift [30], non-Markovian atomic dissipation [38–40] and the decoherence free interatomic interaction [41, 42]. The symmetry bound states outside the band are found numerically for a giant atom coupling to a 1D coupled-resonator waveguide [43]. And the asymmetric bound state close to an atomic transition frequency is found in a giant atom

interacting with the photonic mode of an energy band [44]. In this paper, we study a waveguide quantum electrodynamics system composed of a two-level emitter (TLE) and 1D coupled resonators arranged in a dimer chain due to their alternate on-site photon energies. Different from the 1D coupled-resonator waveguide with uniform-hopping rates, this dimer chain possesses two energy bands, and the TLE non-locally coupled to two adjacent resonators of the dimer chain. To establish the relation of bound states with the mirror symmetry, we present the exact analytical solution of the bound states in real space for arbitrary atomic transition frequency. The asymmetry of bound states stems from the nonlocal coupling of the quantum emitter to two resonators with different on-site energies. Although we show how to judge the symmetry or asymmetry of bound states from the mirror symmetry, the properties of single-photon bound states include more details, for example, how many bound states in this system; whether they all have the same preferred direction or not? Is it possible for a bound state to localized at the one-side of the symmetry axis? How to tune the asymmetry of the bound state?

The paper is organized as follows. In Sec. II, we propose the model describing the interaction between a TLE and a chain of coupled resonators, and the equations of the probability amplitudes are presented in single-excitation subspace. In Sec. III, we derive the condition for the single-photon bound state and discuss the asymmetry of all bound states by introducing the chirality. Finally, a summary has been made in Sec. IV.

II. MODEL FOR A QUANTUM EMITTER NONLOCAL COUPLED TO A DIMER CHAIN

We consider a system consisting of a one-dimensional (1D) waveguide and a TLE. The 1D waveguide consists of a series of coupled resonators in which light propagates due to the coupling between the adjacent resonators (see Fig. 1(a)). The system can be implemented by nano-electromechanical res-

* Corresponding author; gongzr@szu.edu.cn

† Corresponding author; zhoulan@hunnu.edu.cn

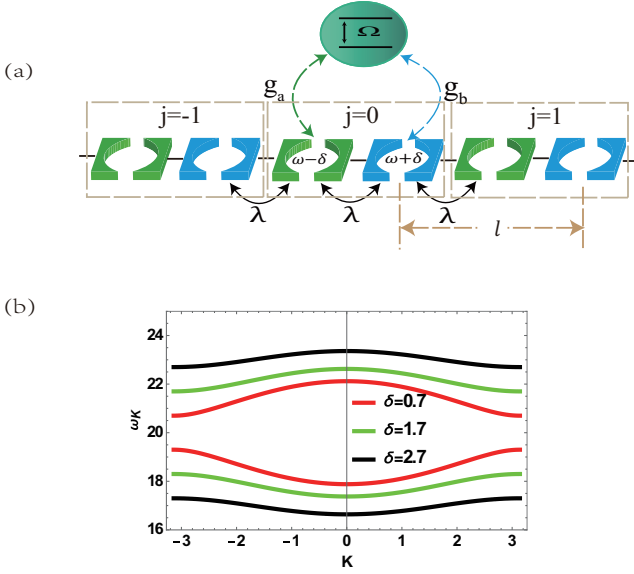


FIG. 1. (Color online) (a) Schematic depiction of a quantum emitter nonlocal coupled to the nearest resonators in a 1D dimer chain of coupled resonators. Dashed boxes indicate the unit cells. (b) The dispersion relation of the dimer chain for $\delta \neq 0$.

onator arrays where two nearest resonators with ferro-magnetic particles in the tips are coupled to a localized spin [45], a side-defected cavity with double couplings to a waveguide of coupled defected cavity arrays [46–48], or a superconducting atoms coupled to a Josephson photonic-crystal waveguide [44, 49]. In contrast to the previous 1D waveguide with identical resonators [5], the two adjacent resonators (shown as the green and blue cavities in Fig 1(a)) have on-site photon energies $\omega_c - \delta$ and $\omega_c + \delta$, respectively. Here, 2δ denotes the energy differences of single photon in the adjacent resonators. We cast this 1D waveguide as a dimer chain of discrete bosonic sites with equally spaced sites but two kinds of on-site photon energies, and the dimer chain is assumed to be infinitely long in both direction. Then the continuum of modes in the waveguide are the Bloch modes. We use \hat{a}_{2j} (\hat{a}_{2j}^\dagger) and \hat{b}_{2j+1} (\hat{b}_{2j+1}^\dagger) as the bosonic annihilation (creation) operators of a single photon for the green and blue resonators at the j th cell, respectively. Its corresponding real-space Hamiltonian reads

$$\begin{aligned} \hat{H}_c = & (\omega_c - \delta) \sum_{j=-\infty}^{+\infty} \hat{a}_{2j}^\dagger \hat{a}_{2j} + (\omega_c + \delta) \sum_j \hat{b}_{2j+1}^\dagger \hat{b}_{2j+1} \\ & - \sum_j \lambda (\hat{a}_{2j}^\dagger \hat{b}_{2j+1} + \hat{a}_{2j}^\dagger \hat{b}_{2j-1}) + h.c. \end{aligned} \quad (1)$$

where λ is the coupling constant between adjacent resonators in the dimer chain. Two bands of propagating photons have the following dispersion relation as

$$\omega_k^\pm = \omega_c \pm \sqrt{\delta^2 + 4\lambda^2 \cos^2(k/2)}. \quad (2)$$

with wave number $k \in [-\pi, \pi]$. The bands of propagating photons with different δ in the first Brillouin zone is depicted

in Fig. 1(b). The time-reversal symmetry is satisfied for the propagating modes in the dimer chain since $\omega_{-k}^\pm = \omega_k^\pm$.

The TLE's ground and excited states $|g\rangle$ and $|e\rangle$, respectively, are separated in energy by Ω . The transition $|g\rangle \leftrightarrow |e\rangle$ of the TLE is dipole coupled with coupling strength g_a (g_b) to the resonator at the 0th cell. Defining the rising operators $\hat{\sigma}_+ = |e\rangle\langle g|$, and its adjoint $\hat{\sigma}_-$, the Hamiltonian for the free TLE part and the interaction between the TLE and the field within the rotating-wave approximation reads

$$\hat{H}_1 = \Omega |e\rangle\langle e| + \hat{\sigma}_+ (g_a \hat{a}_0 + g_b \hat{b}_1) + h.c. \quad (3)$$

Here, we have introduced the nonlocal interaction between the TLE and the light field.

The number operator $\hat{N} = \sum_j (\hat{a}_{2j}^\dagger \hat{a}_j + \hat{b}_{2j+1}^\dagger \hat{b}_{2j+1}) + |e\rangle\langle e|$ commutes with the total Hamiltonian $\hat{H} = \hat{H}_c + \hat{H}_1$. We restrict the analysis to the subspaces with single excitation hereafter. In the single-excitation subspace, there are two mutual exclusive possibilities: the particle either is propagating inside the cavity or is absorbed by the TLE. Letting $|\emptyset\rangle = |0g\rangle$ be the state without photon while the TLE stays on its ground state, the eigenstate of the Hamiltonian reads

$$|\epsilon\rangle = \left(\sum_j \alpha_{2j} \hat{a}_{2j}^\dagger + \sum_j \beta_{2j+1} \hat{b}_{2j+1}^\dagger + u_e \hat{\sigma}_+ \right) |\emptyset\rangle, \quad (4)$$

where $\alpha_{2j}, \beta_{2j+1}$ are the probability amplitudes to find a photon in a and b resonators of the j th cell, respectively, and u_e is the probability amplitude of the TLE in the excited state while no photon in the dimer chain. From the stationary Schrödinger equation, one can obtain the equations for the amplitudes. By removing u_e , the equations for the photonic amplitudes reduce to

$$(\epsilon - \omega_c + \delta) \alpha_{2j} \quad (5a)$$

$$= -\lambda (\beta_{2j+1} + \beta_{2j-1}) + \delta_{j0} (V_a \alpha_0 + G \beta_1),$$

$$(\epsilon - \omega_c - \delta) \beta_{2j+1} \quad (5b)$$

$$= -\lambda (\alpha_{2j} + \alpha_{2j+2}) + \delta_{j0} (G^* \alpha_0 + V_b \beta_1),$$

which lead to a nonlocal energy-dependent delta-like potentials V_n , $n = a, b$ and the effective dispersive coupling strength

$$V_n = \frac{g_n^* g_n}{\epsilon - \Omega}, G = \frac{g_a^* g_b}{\epsilon - \Omega}. \quad (6)$$

Obviously, the effective dispersive coupling strength G vanishes when the TLE only interacts with one resonator of the unit cell, which plays an important role in the emergence of the chiral bound states.

III. SINGLE-PHOTON BOUND STATES

The presence of the TLE breaks down the translational symmetry of the dimer chain, which leads to the highly-localized states. We plot the energy spectrum versus coupling strengths in the single excitation subspace in Fig. 2 by numerical diagonalization of the Hamiltonian in the real space

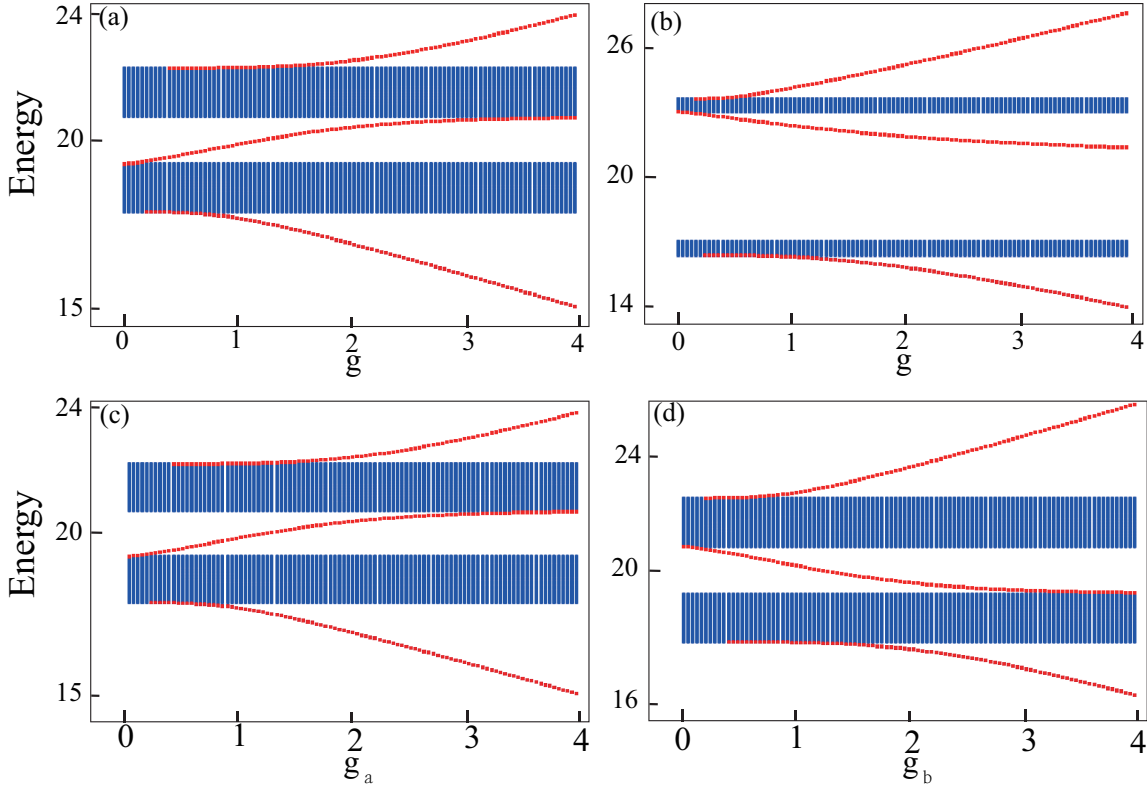


FIG. 2. (Color online) The energy versus coupling strength $g_a = g_b = g$ in (a) and (b), g_a in (c) and g_b in (d) for $\omega_c = 20$. The other parameters are setting as follow: (a) $\delta = 0.7, \Omega = 19.3$, (b) $\delta = 3, \Omega = 23$, (c) $g_b = 0, \delta = 0.7, \Omega = 19.3$, (d) $g_a = 0, \delta = 0.7, \Omega = 20.7$. All parameters are in units of the hop strength λ .

with 100 resonators. The periodic boundary conditions is used. Two energy bands of scattering states are symmetrically formed above and below $\epsilon = \omega_c$ with 2δ as the band gap. Obviously, the two bands merge to one band when there is no energy difference between resonators ($\delta = 0$). The three curves, one above all bands, one below all bands and the other inside the band gap, are the bound states. As coupling strengths increase, the energy differences between the bound states and the band edges also increase. However, the increment of the energy differences between the bound states and the band edges is dependent on transition frequency Ω , especially for the emerging bound state inside the gap. When $\Omega < \omega_c$, the energy of the emerging bound state increases as the coupling strengths increase. When $\Omega > \omega_c$, the energy of the emerging bound state decreases as the coupling strengths increase. In Fig. 2(c) and (d) the TLE only interacts with one resonator of the unit cell. It is noted that Fig.2(d) can be obtained by the mirror reflection of the Fig.2(c) with mirror surface locating at $\epsilon = \omega_c$, which actually indicates the same mirror reflection symmetry of the dimer resonator energies and the TLE's energy when $a \rightarrow b$ and $\Omega - \omega_c \rightarrow -(\Omega - \omega_c)$. Hereafter, for brevity, the bound state above, below the bands are denoted bound state I, II, and the bound state in the band gap is denoted as bound state III.

The highly-localized states in previous studies [10–16, 43]

decay exponentially and symmetrically in both directions, actually, the symmetry of the bound state is guaranteed by the mirror reflection symmetry around the quantum emitter. However, the mirror reflection symmetry is broken in our model with all $g_n \neq 0$. Since only the energy bands are modified, there should still be localized modes of photons around the cell where the TLE is embedded. So we assume the following damped wave

$$\alpha_{2j} = \begin{cases} A_L^\kappa e^{ik_0 j + \kappa j}, & j < 0 \\ A_R^\kappa e^{ik_0 j - \kappa j}, & j > 0 \end{cases} \quad (7a)$$

$$\beta_{2j+1} = \begin{cases} B_L^\kappa e^{ik_0 j + \kappa(j+1/2)}, & j < 0 \\ B_R^\kappa e^{ik_0 j - \kappa(j+1/2)}, & j > 0 \end{cases} \quad (7b)$$

with $k_0 = 0, \pi$, which decreases exponentially with the distance from the 0th cell. The imaginary wave vector $\kappa > 0$ labels the energy

$$\epsilon = \omega_c \pm \sqrt{\delta^2 + \lambda^2 (2 + e^{ik_0 + \kappa} + e^{-ik_0 - \kappa})} \quad (8)$$

of a localized photon outside of the bands. At the region far away from the TLE, we obtain

$$\frac{A_L^\kappa}{B_L^\kappa} = -\lambda \frac{e^{\kappa/2} + e^{-ik_0 - \kappa/2}}{\epsilon - \omega_c + \delta}, \quad \frac{A_R^\kappa}{B_R^\kappa} = -\lambda \frac{e^{-ik_0 + \kappa/2} + e^{-\kappa/2}}{\epsilon - \omega_c + \delta}, \quad (9)$$

By applying Eqs.(7) and (9) to the discrete scattering equation at $j = \pm 1$, the amplitudes for the $j = 0$ cell can be obtained as

$$\alpha_0 = A_L^\kappa, \beta_1 = B_R^\kappa e^{-\kappa/2}. \quad (10)$$

Substituting Eq.(10) and the spatial exponential-decay solution (7) to Eq. (5) at $j = 0$ yields the condition for the energy of the bound state

$$|G - \lambda|^2 = \left(\epsilon - \omega_c + \delta - V_a + \lambda \frac{B_L^\kappa}{A_L^\kappa} e^{-ik_0 - \kappa/2} \right) \times \left(\epsilon - \omega_c - \delta - V_b + \lambda \frac{A_R^\kappa}{B_R^\kappa} e^{ik_0 - \kappa/2} \right) \quad (11)$$

Once κ is obtained from Eq.(11), so does the ratio in Eq.(9). To give an intuitional knowledge on the bound state, we rewrite the wave function of the bound states as

$$\frac{\alpha_{2j}}{A_R^\kappa} = \begin{cases} \frac{A_L^\kappa}{A_R^\kappa} e^{ik_0 j + \kappa j}, & j < 0 \\ \frac{A_L^\kappa}{A_R^\kappa}, & j = 0 \\ e^{ik_0 j - \kappa j}, & j > 0 \end{cases} \quad (12a)$$

$$\frac{\beta_{2j+1}}{A_R^\kappa} = \begin{cases} \frac{A_L^\kappa B_L^\kappa}{A_R^\kappa A_L^\kappa} e^{ik_0 j + \kappa(j+1/2)}, & j < 0 \\ \frac{B_R^\kappa}{A_R^\kappa} e^{-\kappa/2}, & j = 0 \\ \frac{B_R^\kappa}{A_R^\kappa} e^{ik_0 j - \kappa(j+1/2)}, & j > 0 \end{cases} \quad (12b)$$

where the ratio

$$\frac{A_L^\kappa}{A_R^\kappa} = \frac{\lambda}{\lambda - G^*} - \frac{V_b e^{-\kappa/2}}{(G^* - \lambda)} \frac{B_R^\kappa}{A_R^\kappa}. \quad (13)$$

When $k_0 = 0$, Eq.(11) gives the energy $\epsilon_0^\pm = \omega_c \pm \sqrt{\delta^2 + 4\lambda^2 \cosh^2(\kappa/2)}$ lying upper or below all the bands, respectively. When $k_0 = \pi$, Eq.(11) shows that the energy $\epsilon_m^\pm = \omega_c \pm \sqrt{\delta^2 - 4\lambda^2 \sinh^2(\kappa/2)}$ is inside the band gap. The ratios in Eq.(9) indicate that

$$\frac{A_L^\kappa}{B_L^\kappa} = \frac{A_R^\kappa}{B_R^\kappa} \text{ for } k_0 = 0 \quad (14a)$$

$$\frac{A_L^\kappa}{B_L^\kappa} = -\frac{A_R^\kappa}{B_R^\kappa} \text{ for } k_0 = \pi \quad (14b)$$

When the TLE only couples to the resonator at the 0th site, $A_L^\kappa/A_R^\kappa = e^{-ik_0}$. When TLE only couples to the resonator at the 1th site, $A_L^\kappa/A_R^\kappa = e^{-ik_0 + \kappa}$. In Fig. 3, we have plotted the photonic probability distribution of the bound state I (a,d,g), III (b,e,h) and II (c,f,i). It can be found from Fig. 3(a-f) that all the bound states are symmetry about the symmetry axis x_0 . For different coupling situations, the position of the symmetry axis x_0 is different. When the TLE only interacts with single resonator, the same mirror reflection symmetry of the dimer resonator energies and the TLE's energy under $a \rightarrow b$ and $\Omega - \omega_c \rightarrow -(\Omega - \omega_c)$ still can be found in panels (a-c) and (d-f) (e.g. Fig. 3(a) and Fig. 3(f)). However, when the TLE interacts with two adjacent resonators at one unit cell, the bound states no longer has the mirror reflection symmetry as shown in Fig. 3(g-i).

If the TLE is located at the middle of the unit cell at $j = 0$, e.g. position $x_0 = l/4$, the line at the TLE's location divides the space into left- and right-hand side of the TLE. The photonic component of the bound state in Fig. 3(g) are strongly localized at the right-hand side of the TLE, and that in Fig. 3(h) mostly distributes to the left-hand side of the TLE, the asymmetry of the photonic probability on both side of the x_0 axis can also be found in Fig. 3(i). According to the reflection symmetry in geometry, we introduce the chirality [44]

$$S = \frac{S_L - S_R}{S_L + S_R} \quad (15)$$

to depict the asymmetry of the bound state in left- and right-hand side of the TLE

$$S_L = \sum_{j=-1}^{-\infty} (|\alpha_{2j}|^2 + |\beta_{2j+1}|^2) + |\alpha_0|^2, \quad (16a)$$

$$S_R = \sum_{j=1}^{\infty} (|\alpha_{2j}|^2 + |\beta_{2j+1}|^2) + |\beta_1|^2, \quad (16b)$$

where $S > 0$ ($S < 0$) indicates that the left-handed (right-handed) chirality, and $S \rightarrow 1$ ($S \rightarrow -1$) corresponds to the perfect left-handed (right-handed) chirality. By applying the wave function in Eq.(12), we can obtain the expression of the charity in terms of the ratios

$$S = \frac{|A_L^\kappa/A_R^\kappa|^2 + \left(|A_L^\kappa/A_R^\kappa|^2 - 1 \right) \frac{e^{-\kappa} + |B_L^\kappa/A_L^\kappa|^2}{1 - e^{-2\kappa}} e^{-\kappa}}{|A_L^\kappa/A_R^\kappa|^2 + \left(|A_L^\kappa/A_R^\kappa|^2 + 1 \right) \frac{e^{-\kappa} + |B_L^\kappa/A_L^\kappa|^2}{1 - e^{-2\kappa}} e^{-\kappa}} \quad (17)$$

To show the dependence of the chirality on the parameters, we have plotted the chirality S of the bound state versus δ in Fig. 4(a-c) and the coupling strength in Fig. 4(d-f). Since the TLE-resonator coupling strengths are equal in panels (a-c), the break of the reflection symmetry depends on whether δ vanishes or not. It is shown that all chirality vanishes at $\delta = 0$ in panels (a,b) for ordinary bound states I and II. While since the merging bound state III disappear for $\delta = 0$, the critical chirality of the emerging bound state III in panel (c) is quite different for different transition energies of the TLE, while the chirality of ordinary bound states tends to coincidence. One can tune the chirality by adjusting the transition energy Ω for a given δ : the left-handed chirality decreases as Ω increases for bound state II, the right-handed chirality can increase as Ω increases under certain parameters for bound state I. It should be aware that the chirality of bound state I prefers the right-hand side of dimer chain and bound state II prefers the left hand side of dimer chain. Although the chirality of all bound states can be continuously tuned by adjusting δ , the right (left) hand side chirality remains unchanged for bound state I (II), only bound state III can change its sign of chirality for an appropriate Ω (see the green line in panel c). The perfect right (left) chirality can be achieved only for the bound state I (III). For a given δ , one can change the sign of chirality of the bound states I and II by adjusting one of the coupling strengths, see Fig. 4(d) and (e). These changes can be easily explained by following reasons: When $g_b \ll g_a$, bound states are mainly

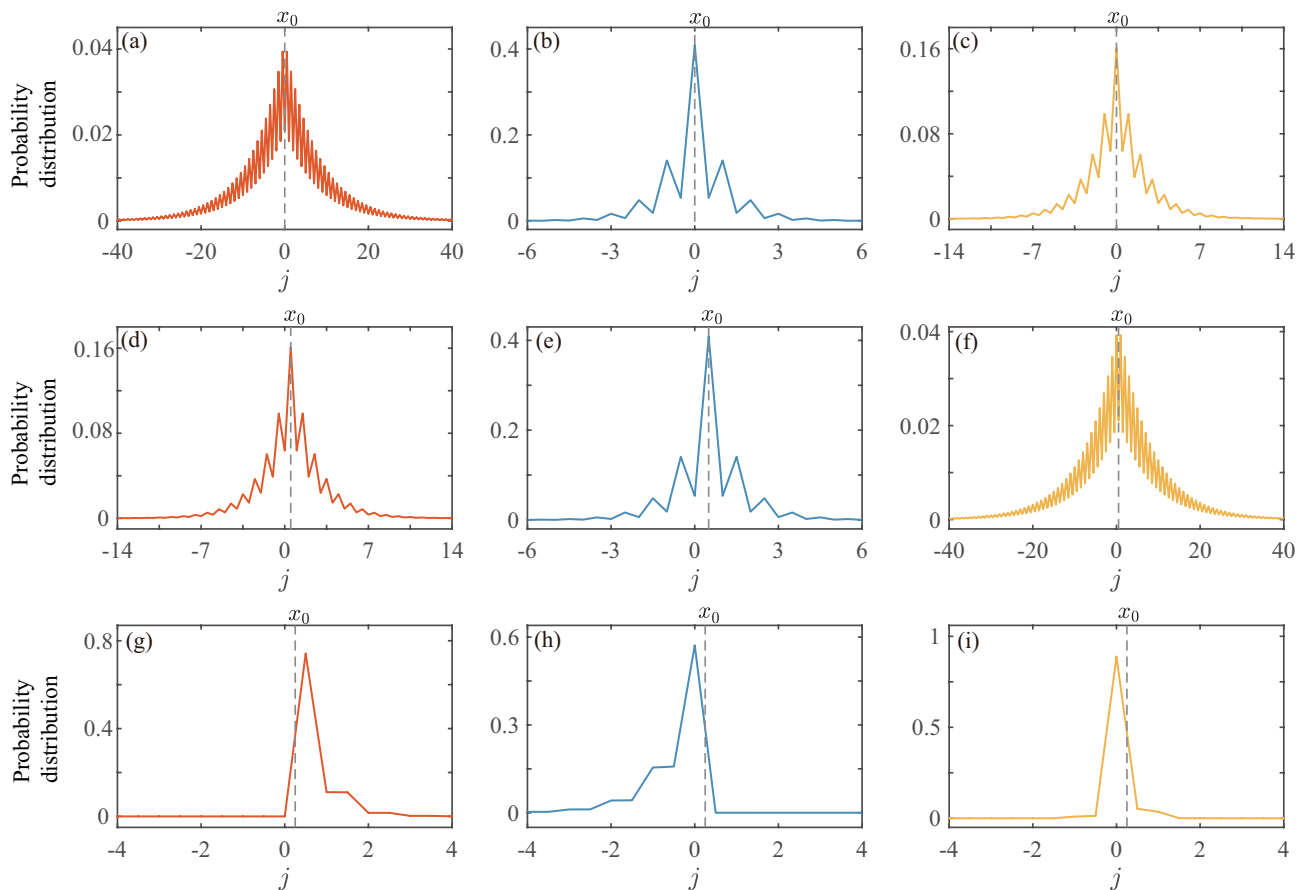


FIG. 3. (Color online) The bound state distribution above all the bands (a,d,g), inside the band gap (b,e,h) and below all the bands (c,f,i). In panels (a-c), $g_a = 0.5, g_b = 0, \delta = 0.7, \Omega = 19.3$, i.e., the TLE only interacts with the resonator at the 0th site. In panels (d-f), $g_a = 0, g_b = 0.5, \delta = 0.7, \Omega = 20.7$, the TLE only interacts with the resonator at the 1th site. In panels (g-i), the TLE interacts with the adjacent resonators at the 0th cell, $g_a = g_b = 0.7$, (g) $\Omega = 22, \delta = 1.1$ (h) $\Omega = 19.3, \delta = 0.7$, (i) $\Omega = 15.5, \delta = 3.8$. All parameters are in units of the hop strength λ and $\omega_c = 20$.

localized around the 0th site, however the symmetry line is positioned at $x_0 = l/4$ not $x_0 = 0$, they present left handed chirality; When $g_b \gg g_a$, bound states are mainly localized around the 1th site, thence the symmetry line positioned at $x_0 = l/4$ gives rise to a right handed chirality of bound state I and II. It can be also found that the left handed chirality increases (decreases) as Ω increases when g_b is smaller than g_a and the right handed chirality increases (decreases) as Ω increases when g_b is larger than g_a for bound state I (II), the perfect right (left) charity can be still achieved only for the bound state I (III).

IV. CONCLUSION

In summary, we consider the TLE is coupled to two adjacent resonators, where two resonators in each dimer have different on-site photon energies. In the single-excitation subspace, this system has propagating states forming two energy bands and as well as bound-states. We mainly focus on the chiral feature of the bound states. After obtaining the analytical solutions of the bound states in real space, we found that 1)

the bound-state distributes symmetrically around the coupling point when the TLE is locally coupled to one resonator of the dimer chain; 2) the mirror-reflection symmetry breaking leads to the formation of three chiral bound states when the TLE is nonlocal coupled to two adjacent resonators. The chirality of the bound states inherits from the geometry aspects, which are characterized by either the difference of on-site energies in each unit cell or the coupling strengths between the TLE and the resonators, but it can also be tuned by the transition energy of the TLE. When the coupling strengths are identical, the nonvanishing difference of on-site energies lead to right handed chirality of bound state I and left handed chirality of bound state II, and bound state III can change its preferred chirality by adjusting on-site difference together with appropriate transition energy of the TLE. For given on-site energies, one can change the preferred chirality the bound states I and II by adjusting one of the coupling strengths.

ACKNOWLEDGMENTS

We are grateful to Z.H. Wang for useful discussions.

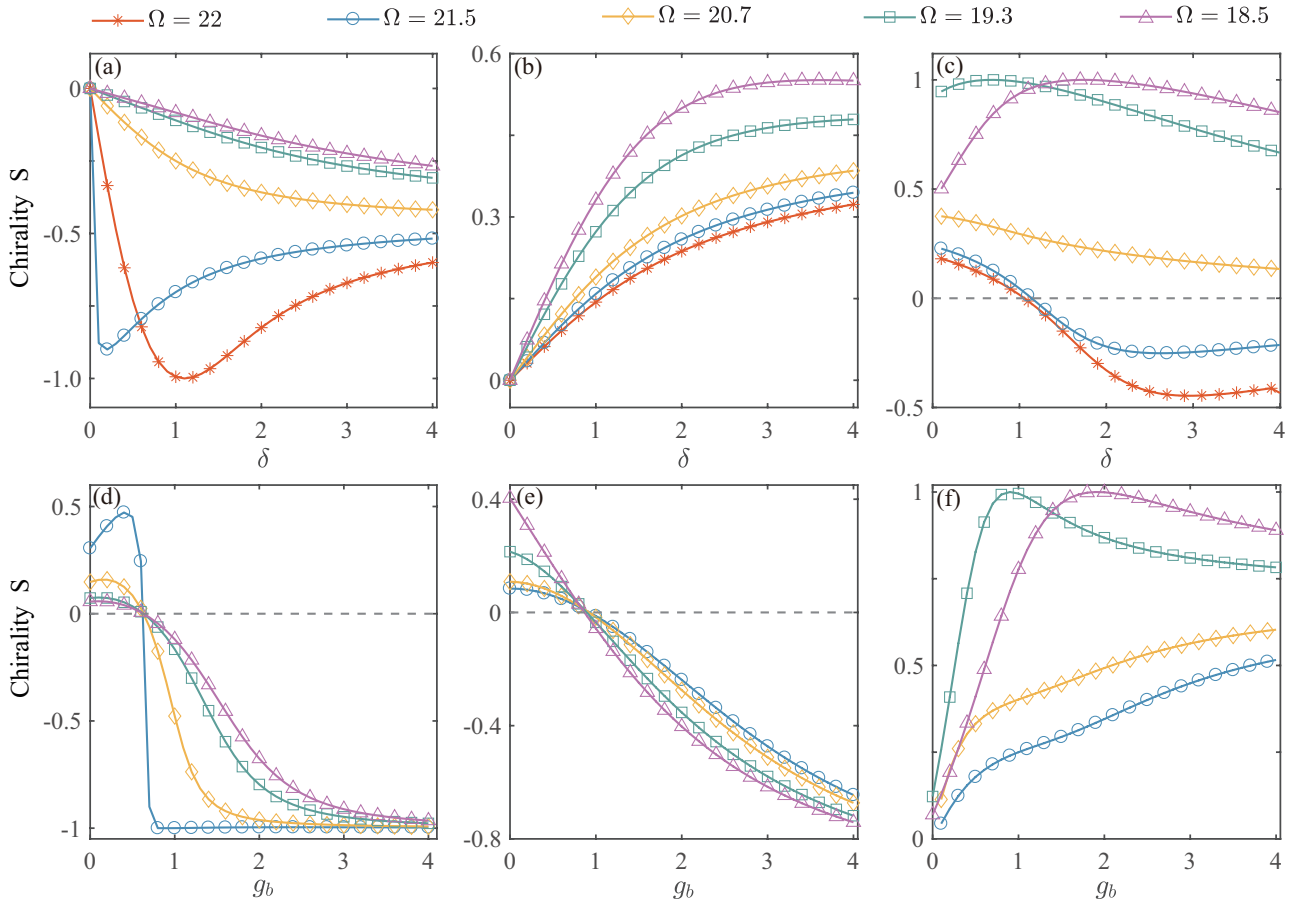


FIG. 4. (Color online) Tuning the chirality of the bound state above all the bands (a,d), below all the bands (b,e) and inside the band gap (c,f). (a)-(c) Chirality versus δ for fixed coupling strength $g_a = g_b = 0.7$, and $\Omega = 22$ (red), $\Omega = 21.5$ (blue), $\Omega = 20.7$ (yellow), $\Omega = 19.3$ (green) and $\Omega = 18.5$ (purple). (d)-(f) Chirality versus g_b for fixed $\delta = 0.2$, $g_a = 0.7$, $\Omega = 21.5$ (blue), $\Omega = 20.7$ (yellow), $\Omega = 19.3$ (green) and $\Omega = 18.5$ (purple). All parameters are in units of the hop strength λ and $\omega_c = 20$.

This work was supported by NSFC Grants No. 11975095, No. 12075082, No.11935006, No. 12175150, the science and

technology innovation Program of Hunan Province (Grant No. 2020RC4047) and the Natural Science Foundation of Guangdong Province (Grant No. 2019A1515011400).

-
- [1] X. Gu, A. F. Kockum, A. Miranowicz, Y.-X. Liu, and F. Nori, Microwave photonics with superconducting quantum circuits, *Phys. Rep.* **718**, 1 (2017).
- [2] D. Roy, C. M. Wilson, and O. Firstenberg, Colloquium: Strongly interacting photons in one-dimensional continuum, *Rev. Mod. Phys.* **89**, 021001 (2017).
- [3] A.S. Sheremet, M. I. Petrov, I. V. Iorsh, A. V. Poshakinskiy, and A. N. Poddubny, Waveguide quantum electrodynamics: Collective radiance and photon-photon correlations, *Rev. Mod. Phys.* **95**, 015002 (2023).
- [4] J. T. Shen and S. Fan, Coherent Single Photon Transport in a One-Dimensional Waveguide Coupled with Superconducting Quantum Bits, *Phys. Rev. Lett.* **95**, 213001 (2005).
- [5] L. Zhou, Z. R. Gong, Y.-x. Liu, C. P. Sun and F. Nori, Controllable Scattering of a Single Photon inside a One-Dimensional Resonator Waveguide, *Phys. Rev. Lett.* **101**, 100501 (2008).
- [6] L. Zhou, H. Dong, Y.-x. Liu, C. P. Sun, and F. Nori, Quantum supercavity with atomic mirrors, *Phys. Rev. A* **78**, 063827 (2008);
- [7] Z. R. Gong, H. Ian, L. Zhou, and C. P. Sun, Controlling quasibound states in a one-dimensional continuum through an electromagnetically-induced-transparency mechanism, *Phys. Rev. A* **78**, 053806 (2008).
- [8] H. Dong, Z. R. Gong, H. Ian, Lan Zhou, and C. P. Sun, Intrinsic cavity QED and emergent quasinormal modes for a single photon, *Phys. Rev. A* **79**, 063847 (2009).
- [9] T. Tufarelli, F. Ciccarello, and M. S. Kim, Dynamics of spontaneous emission in a single-end photonic waveguide, *Phys. Rev. A* **87**, 013820 (2013).
- [10] L. Zhou, S. Yang, Y.-x. Liu, C. P. Sun, and F. Nori, Quantum Zeno switch for single-photon coherent transport, *Phys. Rev. A* **80**, 062109 (2009).

- [11] Paolo Longo, Peter Schmitteckert and Kurt Busch, Few-Photon Transport in Low-Dimensional Systems: Interaction-Induced Radiation Trapping, *Phys. Rev. Lett.* 104 023602 (2010).
- [12] L. Zhou, L. P. Yang, Y. Li, and C. P. Sun, Quantum Routing of Single Photons with a Cyclic Three-Level System, *Phys. Rev. Lett.* **111**, 103604 (2013).
- [13] J. Lu, L. Zhou, L.-M. Kuang, and F. Nori, Single-photon router: Coherent control of multichannel scattering for single photons with quantum interferences, *Phys. Rev. A* **89**, 013805 (2014).
- [14] F. Lombardo, F. Ciccarello and G. M. Palma, Photon localization versus population trapping in a coupled-cavity array, *Phys. Rev. A* **89**, 053826 (2014).
- [15] E. Sánchez-Burillo, D. Zueco, L. Martín-Moreno, and J. J. García-Ripoll, Dynamical signatures of bound states in waveguide QED, *Phys. Rev. A* **96**, 023831 (2017).
- [16] M. Ahumada, P. A. Orellana, and J. C. Retamal, Bound states in the continuum in whispering gallery resonators, *Phys. Rev. A* **98**, 023827 (2018).
- [17] J. T. Shen and S. Fan, Strongly Correlated Two-Photon Transport in a One-Dimensional Waveguide Coupled to a Two-Level System, *Phys. Rev. Lett.* **98**, 153003 (2007).
- [18] H.X. Zheng, D. J. Gauthier, and H. U. Baranger, Waveguide QED: Many-body bound-state effects in coherent and Fock-state scattering from a two-level system, *Phys. Rev. A* **82**, 063816 (2010).
- [19] T. Shi, Shanhui Fan, and C. P. Sun, Two-photon transport in a waveguide coupled to a cavity in a two-level system, *Phys. Rev. A* **84**, 063803 (2011).
- [20] D. Roy, Two-Photon Scattering by a Driven Three-Level Emitter in a One-Dimensional Waveguide and Electromagnetically Induced Transparency, *Phys. Rev. Lett.* **106**, 053601 (2011).
- [21] T. Shi, Y.-H. Wu, A. Gonzalez-Tudela and J. I. Cirac, Bound States in Boson Impurity Models, *Phys. Rev. X* **6**, 021027 (2016).
- [22] L. Qiao, Y.-J. Song and C.-P. Sun, Quantum phase transition and interference trapping of populations in a coupled-resonator waveguide, *Phys. Rev. A* **100**, 013825 (2019).
- [23] L. Zhou, Y. Chang, H. Dong, L.-M. Kuang and C. P. Sun, Inherent Mach-Zehnder interference with "which-way" detection for single-particle scattering in one dimension, *Phys. Rev. A* **85**, 013806 (2012).
- [24] Z. H. Wang, L. Zhou, Y. Li and C. P. Sun, Controllable single-photon frequency converter via a one-dimensional waveguide, *Phys. Rev. A* **89**, 053813 (2014).
- [25] Wei-Bin Yan and Heng Fan, Control of single-photon transport in a one-dimensional waveguide by a single photon, *Phys. Rev. A* **90**, 053807 (2014).
- [26] P. T. Fong and C. K. Law, Bound state in the continuum by spatially separated ensembles of atoms in a coupled-cavity array, *Phys. Rev. A* **96** 023842 (2017).
- [27] Xun-Wei Xu, Ai-Xi Chen, Yong Li and Yu-xi Liu, Single-photon nonreciprocal transport in one-dimensional coupled-resonator waveguides, *Phys. Rev. A* **95** 063808 (2017).
- [28] Zhihai Wang, Lei Du, Yong Li and Yu-xi Liu, Phase-controlled single-photon nonreciprocal transmission in a one-dimensional waveguide, *Phys. Rev. A* **100** 053809 (2019).
- [29] Lei Qiao and Chang-Pu Sun, Atom-photon bound states and non-Markovian cooperative dynamics in coupled-resonator waveguides, *Phys. Rev. A* **100** 063806 (2019).
- [30] A. F. Kockum, P. Delsing, and G. Johansson, Designing frequency-dependent relaxation rates and Lamb shifts for a giant artificial atom, *Phys. Rev. A* **90**, 013837 (2014).
- [31] A. F. Kockum, Quantum optics with giant atoms—the first five years, in *International Symposium on Mathematics, Quantum Theory, and Cryptography*, (Springer, Singapore, 2021), p. 125.
- [32] M. V. Gustafsson, T. Aref, A. F. Kockum, M. K. Ekstrom, G. Johansson and P. Delsing, Propagating phonons coupled to an artificial atom, *Science* **346**, 207-211 (2014).
- [33] R. Manenti, A. F. Kockum, A. Patterson, T. Behrle, J. Rahamim, G. Tancredi, F. Nori and P. J. Leek, Circuit quantum acoustodynamics with surface acoustic waves, *Nat. Commun.* **8**, 975 (2017).
- [34] P. Delsing et al., The 2019 surface acoustic waves roadmap, *J. Phys. D* **52**, 353001 (2019).
- [35] L. R. Sletten, B. A. Moores, J. J. Viennot, and K. W. Lehnert, Resolving Phonon Fock States in a Multimode Cavity with a Double-Slit Qubit, *Phys. Rev. X* **9**, 021056 (2019).
- [36] G. Andersson, M. K. Ekström and P. Delsing, Electromagnetically Induced Acoustic Transparency with a Superconducting Circuit, *Phys. Rev. Lett.* **124**, 240402 (2020).
- [37] A. Bienfait, Y. P. Zhong, H.-S. Chang, M.-H. Chou, C. R. Conner, É. Dumur, J. Grebel, G. A. Peairs, R. G. Povey, K. J. Satzinger and A. N. Cleland, Quantum Erasure Using Entangled Surface Acoustic Phonons, *Phys. Rev. X* **10**, 021055 (2020).
- [38] L. Guo, A. Grimsmo, A. F. Kockum, M. Pletyukhov and G. Johansson, Giant acoustic atom: A single quantum system with a deterministic time delay, *Phys. Rev. A* **95**, 053821 (2017).
- [39] L. Guo, A. F. Kockum, F. Marquardt and G. Johansson, Oscillating bound states for a giant atom, *Phys. Rev. Research* **2**, 043014 (2020).
- [40] G. Andersson, B. Suri, L. Guo, T. Aref and P. Delsing, Non-exponential decay of a giant artificial atom, *Nat. Phys.* **15**, 1123 (2019).
- [41] A. F. Kockum, G. Johansson and F. Nori, Decoherence-Free Interaction between Giant Atoms in Waveguide Quantum Electrodynamics, *Phys. Rev. Lett.* **120**, 140404 (2018).
- [42] A. Carollo, D. Cilluffo and F. Ciccarello, Mechanism of decoherence-free coupling between giant atoms, *Phys. Rev. Research* **2**, 043184 (2020).
- [43] W. Zhao and Z.H. Wang, Single-photon scattering and bound states in an atom-waveguide system with two or multiple coupling points, *Phys. Rev. A* **101**, 053855 (2020).
- [44] X. Wang, T. Liu, A. F. Kockum, H.-R. Li and F. Nori, Tunable Chiral Bound States with Giant Atoms, *Phys. Rev. Lett.* **126** 043602 (2021).
- [45] P. Rabl, S. J. Kolkowitz, F. H. L. Koppens, J. G. E. Harris, P. Zoller, and M. D. Lukin, A quantum spin transducer based on nanoelectromechanical resonator arrays, *Nat. Phys.* **6**, 602 (2010).
- [46] T. Baba, Slow light in photonic crystals, *Nat. Photon.* **2**, 465 (2008).
- [47] D. Z. Xu, H. Ian, T. Shi, H. Dong, and C. P. Sun, Photonic Feshbach resonance, *Sci. China Phys., Mech. Astron.* **53**, 1234 (2010).
- [48] L. Zhou, Y. Chang, H. Dong, L.-M. Kuang and C. P. Sun, Inherent Mach-Zehnder interference with "which-way" detection for single-particle scattering in one dimension, *Phys. Rev. A* **85**, 013806 (2012).
- [49] Marco Scigliuzzo, Giuseppe Calajò, Francesco Ciccarello, Daniel Perez Lozano, Andreas Bengtsson, Pasquale Scarlino, Andreas Wallraff, Darrick Chang, Per Delsing, and Simone Gasparinetti, Controlling Atom-Photon Bound States in an Array of Josephson-Junction Resonators, *Phys. Rev. X* **12**, 031036 (2022)